

Evaluating strong measurement noise in data series with simulated annealing method

J. Carvalho¹, F. Raischel², M. Haase³, P. Lind^{1,2}

¹Departamento de Física, Faculdade de Ciências da Universidade de Lisboa, 1649-003 Lisboa, Portugal

²Center for Theoretical and Computational Physics, University of Lisbon, 1649-003 Lisbon, Portugal

³Institute for High Performance Computing, University of Stuttgart, D-70569 Stuttgart, Germany

E-mail: raischel@ci.fc.ul.pt

Abstract. Many stochastic time series can be described by a Langevin equation composed of a deterministic and a stochastic dynamical part. Such a stochastic process can be reconstructed by means of a recently introduced nonparametric method, thus increasing the predictability, i.e. knowledge of the macroscopic drift and the microscopic diffusion functions. If the measurement of a stochastic process is affected by additional strong measurement noise, the reconstruction process cannot be applied. Here, we present a method for the reconstruction of stochastic processes in the presence of strong measurement noise, based on a suitably parametrized ansatz. At the core of the process is the minimization of the functional distance between terms containing the conditional moments taken from measurement data, and the corresponding ansatz functions. It is shown that a minimization of the distance by means of a simulated annealing procedure yields better results than a previously used Levenberg-Marquardt algorithm, which permits a rapid and reliable reconstruction of the stochastic process.

1. Introduction

Physical systems often can be resolved on two different time scales, observing slowly varying macroscopic motion while much faster microscopic interactions are perceived as an effective noisy driving. An adequate description of these systems can be obtained by a Langevin equation, which yields a deterministic drift term and a stochastic diffusion term. With respect to this description, reconstructing the drift and diffusion terms of an unknown process in time or scale from a data set enables one to enhance the predictability of that process. Recently, a nonparametric method of reconstruction based solely in the measured time series has been suggested [1]. The method has been applied successfully to data sets from fields such diverse as turbulent fluid dynamics [2], human movement [3], financial data [4], climate indices [5, 6], and to electroencephalographic recordings from epilepsy patients [7, 8]. For the case of finite time steps [9, 10], which can occur when the data is not available at sufficiently high sampling rates, recent improvements have been suggested [11, 12, 13].

However, any experimental setup will record additional measurement noise when recording a data series, which cannot be easily distinguished from the intrinsic dynamical noise. The presence of measurement noise can destroy the Markovian properties of the data and lead to incorrect estimates for the drift and diffusion terms [18, 20].

It has been suggested to separate the measurement noise from the dynamics of the measured variable using different predictor models or schemes for noise reduction [14, 15]. Recently, another approach has been suggested, which allows reconstructing the properties of stochastic time series affected by exponentially correlated Gaussian noise, using algebraic properties of the normal distribution [16]. Here, we revisit an approach presented in Refs. [17, 18], which minimizes the functional distance between

characteristic functions extracted from the measurement data and corresponding terms calculated from a suitably parametrized ansatz for the drift and diffusion functions. We show that using a Simulated Annealing (SA) [19] method for the optimization yields results that are superior to the ones obtained previously by means of the Levenberg-Marquardt (LM) method.

We start in Sec. 2 by describing the general framework for extracting the evolution equation of a signal spoiled by strong measurement noise, together with the amplitude of said measurement noise. In Sec. 3 both LM and SA methods are addressed and compared. Section 4 concludes the paper.

2. Langevin approach for data sets with measurement noise

We consider a one-dimensional Langevin process $x(t)$ defined as

$$\frac{dx}{dt} = D_1(x) + \sqrt{D_2(x)}\Gamma_t, \quad (1)$$

where Γ_t represents a Gaussian δ -correlated white noise $\langle \Gamma_t \rangle = 0$ and $\langle \Gamma_t \Gamma_{t'} \rangle = 2\delta(t - t')$. The Kramers-Moyal (KM) functions $D_1(x)$ and $D_2(x)$ are defined as

$$D_n(x) = \frac{1}{n!} \lim_{\tau \rightarrow 0} \frac{1}{\tau} M_n(x, \tau) \quad (2)$$

for $n = 1, 2$, where D_1 describes the deterministic drift and D_2 corresponds to a diffusion process. An estimate of the n -th order conditional moments of the data $M_n(x, \tau)$ can be extracted directly from the measured time series as

$$\hat{M}_n(x_i, \tau) = \langle (x(t + \tau) - x(t))^n \rangle_{|x(t)=x_i}, \quad (3)$$

the hat indicating that they are calculated from the measured data $x(t)$ directly, whereas the brackets $\langle \rangle$ denote averaging over suitable parts of the time series – or ensemble averages, if available – as described in Refs. [1, 4, 6, 17]. Thus, a nonparametric reconstruction of the stochastic process can be achieved.

In the following, we will consider a time series generated by integrating Eq. (1) with drift and diffusion coefficient assumed to be linear and quadratic forms respectively,

$$D_1(x) = d_{10} + d_{11}x \quad (4a)$$

$$D_2(x) = d_{20} + d_{21}x + d_{22}x^2. \quad (4b)$$

Though we concentrate on the particular expressions for D_1 and D_2 given above, it should be stressed that they comprehend a large collection of different processes, such as Ornstein-Uhlenbeck processes [17]. The parameter d_{10} can always be eliminated through a simple transformation $x \rightarrow x' = x + d_{10}/d_{11}$. For the numerical examples in the remainder of the text, we will use the parameters $d_{10} = 1, d_{11} = -1, d_{20} = 1, d_{21} = -1, d_{22} = 1$.

We now consider the case that the signal of $x(t)$ is affected by a Gaussian δ -correlated measurement white noise, which leads to the series of observations

$$y(t) = x(t) + \sigma\zeta(t) \quad (5)$$

where σ denotes the amplitude of the measurement noise. As Figs. 1a and 1b show, although the trend of $x(t)$ is still visible in the presence of measurement noise, it is intuitively difficult to distinguish between the intrinsic dynamic noise and the measurement noise. Likewise, Fig. 1c illustrates that for increasing σ one obtains broader probability density functions $P(y)$: the standard deviation of these distribution increases with the measurement noise, whereas the mean value remains constant.

In the presence of measurement noise, the conditional moments yield non-zero finite values at $\tau = 0$ and thus the limit $\lim_{\tau \rightarrow 0} \frac{1}{\tau} \hat{M}_n(x, \sigma \neq 0, \tau)$ does not exist [18]. Likewise, the requirements for Markovianity of the measured time series $y(t)$ may not be satisfied [20].

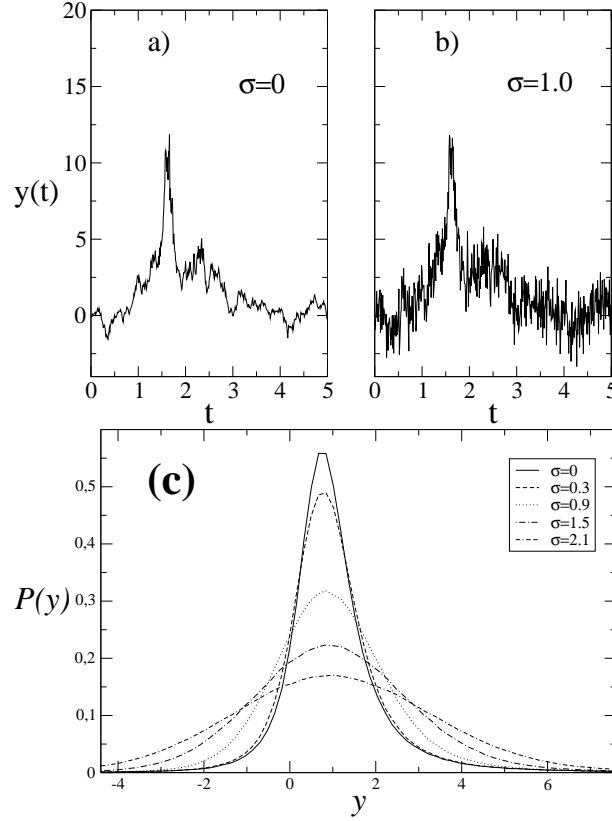


Figure 1. Langevin time series with different measurement noise strengths. Here we show a time series **(a)** without measurement noise, and **(b)** with strong measurement noise. In **(c)** the probability density function $P(y)$ of the series with measurement noise (see Eq. (5)) is shown. In all cases, the assumed time series $x(t)$ without measurement noise uses the coefficients $D_1(x) = 1 - x$ and $D_2(x) = 1 - x + x^2$, when integrating Eq. (1).

However, the two conditional moments [1, 4, 6, 17, 18] $\hat{M}_n(y_i, \tau)$ ($n = 1, 2$) can be derived taking $y(t)$ instead of $x(t)$ in Eq. (3). Figure 2 shows plots of both conditional moments as a function of τ for different strengths of the measurement noise. The linear dependence of M_1 and M_2 on τ makes it still possible to obtain an estimate for the ‘spoiled’ KM-coefficients:

$$\hat{D}_n(y) = \frac{\hat{M}_n(y, \tau_2) - \hat{M}_n(y, \tau_1)}{n!(\tau_2 - \tau_1)}. \quad (6)$$

Within this description, an estimate for the amplitude of the measurement noise yields $\sigma \approx \sqrt{\frac{\hat{M}_2(\mu, 0)}{2}}$ (see Ref. [17, 21]), where μ is the average value of $y(t)$ data points in the time series. As shown in Fig. 2c, such an estimate is not valid for sufficiently strong measurement noise, i. e. $\sigma \gtrsim 0.5$.

The coefficients D_1 and D_2 cannot be correctly estimated, though. Figure 3 shows how the estimated parameters \hat{d}_{ij} deviate from the ‘true’ values d_{ij} of the process given by Eq. (4) as measurement noise increases. Notice that for $\sigma = 0$ (left vertical axis in each plot of Fig. 3) the estimated parameter values are approximately correct.

To correctly derive the drift and diffusion coefficients $D_1(x)$ and $D_2(x)$ when σ is strong, we consider the measured conditional moments $\hat{M}_1(y_i, \tau)$ and $\hat{M}_2(y_i, \tau)$. Since these conditional moments depend

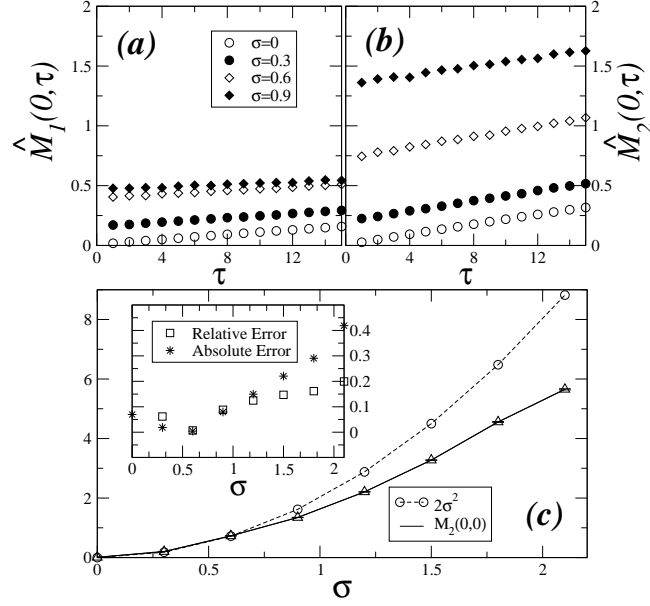


Figure 2. Conditional moments (a) $\hat{M}_1(y_i, \tau)$ and (b) $\hat{M}_2(y_i, \tau)$ as a function of τ , for bin $y_i = 0$ and different measurement noise strengths σ . The same $x(t)$ as in Fig. 1 was used. (c) First estimate of the measurement noise (see text).

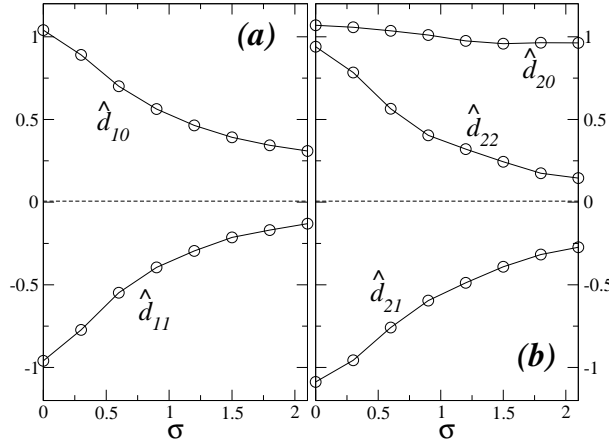


Figure 3. Noise dependence of functions $\hat{D}_1(y)$ and $\hat{D}_2(y)$ (see text and Eq. (6)). The underlying Langevin time series $x(t)$ without noise is the same as in Fig. 1.

in a non-trivial way on both time τ and amplitude y_i , we approximate them up to first order on τ :

$$\hat{M}_1(y_i, \tau) = \langle y(t + \tau) - y(t) \rangle|_{y(t)=y_i} = \tau \hat{m}_1(y_i) + \hat{\gamma}_1(y_i) + \mathcal{O}(\tau^2), \quad (7a)$$

$$\hat{M}_2(y_i, \tau) = \langle (y(t + \tau) - y(t))^2 \rangle|_{y(t)=y_i} = \tau \hat{m}_2(y_i) + \hat{\gamma}_2(y_i) + \sigma^2 + \mathcal{O}(\tau^2), \quad (7b)$$

where $y(t)$ is taken in the range $y_i \pm \Delta y/2$ for each bin i , and Δy depends on the binning considered.

While the functions \hat{m}_i and $\hat{\gamma}_i$ ($i = 1, 2$) are obtained explicitly for each bin value y_i , the decisive aspect of this approach is the fact that the ansatz functions m_i and γ_i can be calculated from the drift and

diffusion coefficients D_1, D_2 and the measurement noise distribution f_σ as follows [18]:

$$\gamma_1(y) = \int_{-\infty}^{+\infty} (x - y) \bar{f}_\sigma(x|y) dx \quad (8a)$$

$$\gamma_2(y) = \int_{-\infty}^{+\infty} (x - y)^2 \bar{f}_\sigma(x|y) dx \quad (8b)$$

$$m_1(y) = \int_{-\infty}^{+\infty} D_1(x) \bar{f}_\sigma(x|y) dx \quad (8c)$$

$$m_2(y) = 2 \int_{-\infty}^{+\infty} [(x - y)D_1(x) + D_2(x)] \bar{f}_\sigma(x|y) dx, \quad (8d)$$

where $\bar{f}_\sigma(x|y)$ is the probability for the system to adopt the value x if a measured value y is observed.

The problem we then solve is to parametrize D_1, D_2 and the noise strength σ and to determine the set of parameters that minimize the functional distance F between the measured functions $\hat{m}_i, \hat{\gamma}_i$ and their counterparts m_i, γ_i defined as

$$F = \frac{1}{M} \sum_{i=1}^M \left[\frac{(\hat{\gamma}_1 - \gamma_1(y_i))^2}{\sigma_{\hat{\gamma}_1}^2(y_i)} + \frac{(\hat{\gamma}_2 - \gamma_2(y_i) - \sigma^2)^2}{\sigma_{\hat{\gamma}_2}^2(y_i)} + \frac{(\hat{m}_1 - m_1(y_i))^2}{\sigma_{\hat{m}_1}^2(y_i)} + \frac{(\hat{m}_2 - m_2(y_i))^2}{\sigma_{\hat{m}_2}^2(y_i)} \right], \quad (9)$$

where the summation extends over all M bins, and $\sigma_{\hat{\gamma}_1}(y_i)$ is the error associated to function $\hat{\gamma}_1$ at the value y_i (and similarly for $\sigma_{\hat{\gamma}_2}, \sigma_{\hat{m}_1}$ and $\sigma_{\hat{m}_2}$, all of them taken directly from the data only).

After computing the functions $\hat{\gamma}_1, \hat{\gamma}_2$, we start from the initially estimated set of values for the parameters and iteratively improve the solution by seeking lower values of F , until convergence is attained. In the following section we use two different methods for minimizing the functional F , namely the LM method [18] and SA method. We will show that for our purposes SA is significantly better than LM.

3. Comparing two optimization methods: Levenberg-Marquardt and Simulated Annealing

In this section, we consider the parameters $\sigma, d_{11}, d_{20}, d_{21}$ and d_{22} which we denoted as p_k with $k = 1, \dots, 5$, respectively. For the Levenberg-Marquardt procedure one computes the derivatives of F with respect to the parameters $\mathbf{p} = \{p_k\}$, and uses them to define the coefficients $\beta_k = \frac{1}{2} \frac{\partial F}{\partial p_k}$ and $\alpha_{kl} = \sum_{j=1}^4 \sum_{i=1}^M \frac{1}{\sigma_j^2(y_i)} \frac{\partial f_j(y_i, \mathbf{p})}{\partial p_k} \frac{\partial f_j(y_i, \mathbf{p})}{\partial p_l}$, where $f_j(y_i, \mathbf{p})$ is the j -th summand in the bracketed inner sum defining F , Eq. (9). The descent δp_l is computed from $\sum_{l=1}^M \alpha'_{kl} \delta p_l = \beta_k$, which uses a damped version of the Gaussian matrix:

$$\alpha'_{kl} = \begin{cases} \alpha'_{kl} = (1 - \lambda) \alpha_{kl}, & k = l \\ \alpha'_{kl} = \alpha_{kl}, & k \neq l \end{cases} \quad (10)$$

The parameter λ is updated during the optimization. The procedure stops after sufficient convergence has been achieved. For details, see Ref. [22]. We generated several data sets from Eq. (1) with different 'input' measurement noise amplitudes $0 < \sigma_I \leq 1.2$, in order to compare the reconstructed parameters to the actual values.

The optimization results are shown in Fig. 4, triangles indicating the first estimate for the parameter values (see Sec. 2), solid lines indicating the true values used to generate the data, and squares indicating the value after LM-optimization.

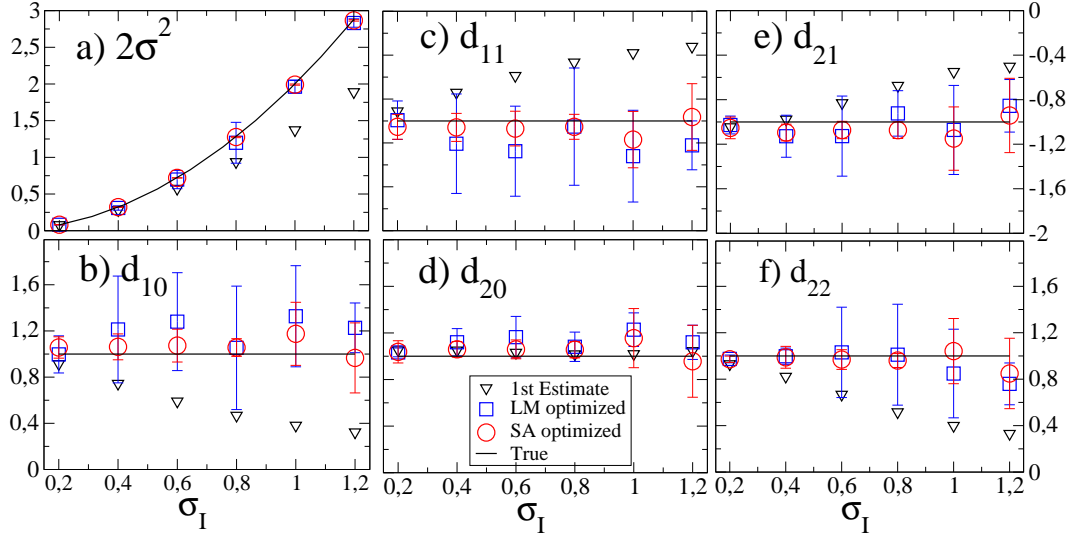


Figure 4. Comparison of the optimized parameters values (bullet) with the first estimate and the true values for different input measurement noise strengths σ_I : **(a)** $2\sigma^2$, **(b)** d_{10} , **(c)** d_{11} , **(d)** d_{20} , **(e)** d_{21} , **(f)** d_{22} . The measurement noise is correctly extracted, as well as the parameters representing the drift coefficient $D_1(x)$ and the diffusion coefficient $D_2(x)$. SA results are significantly better than LM results (see text). Error bars represent the maximum and minimum values encountered in 10 realizations.

While the parameters are well estimated, particularly the magnitude of measurement noise and the drift parameters d_{10} and d_{11} , it was found that LM sometimes does not converge, or converges to a local minimum, the latter fact becoming visible when comparing the results after starting from different initial values. Both these shortcomings required that the LM optimization results were drawn as the best results of a series of attempts with different starting values. The intent to overcome these shortcomings led us to attempt the SA method (squares in Fig. 4).

Simulated annealing is a probabilistic global optimization method. Starting from initial guesses for the parameter vector it proceeds with a step in a random direction. The step is accepted immediately if the energy function at the new position F_{new} (see Eq. (9)) is lower than the previous energy F_{old} , or it is accepted with a probability given by a Boltzmann factor $\exp(-\Delta F/kT)$, where $\Delta F = F_{\text{new}} - F_{\text{old}}$. Otherwise the step is refused and a new parameter step is chosen. This procedure corresponds to the motion of thermal atoms in an attractive potential. Gradual cooling is then achieved by reducing the temperature parameter, thus annealing the test particle in the minimum of the energy landscape.

Figure 4 shows that both optimization methods determine the value of input measurement noise σ_I correctly in all cases, which we find remarkable given the comparable magnitude of measurement noise and the time series $x(t)$ for $\sigma \approx 1$. Furthermore, it can be seen that both LM and SA estimate the parameters d_{1k} for the drift and d_{2l} for the diffusion coefficient correctly; as expected [18], the drift coefficients are determined with higher precision. In general, the SA routine provides more accurate results than LM.

In the LM case, for stronger measurement noise amplitudes, namely for $\sigma > 1.2$, the algorithm is sometimes stuck in a local minimum of the function F , leading to unreliable coefficients d_{ik} . The same set of 10 time series with 10^6 data points were used for each method, but in the LM case, not all cases showed local minima sufficiently close to the true parameter values. Therefore, in our comparison, we overestimate the best performance of the LM method, by considering only the best five cases out of the set of 10 time series (squares in Fig. 4).

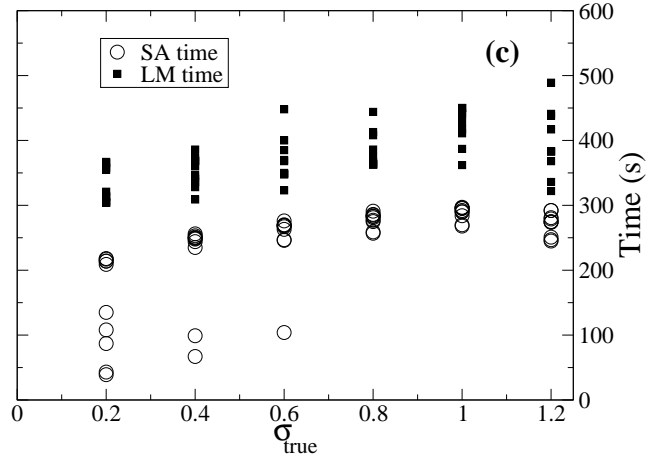


Figure 5. (a) Plot of the relative energy in comparison to the true value, Eq.(11), as a function of the Euclidean distance $dr = ||p_i - p_{i,0}||_2$ of the parameters from the true parameter values $\{p_{i,0}\}$ found with SA method (circles) and with the LM method (squares) for $\sigma = 1.2$. (b) Close-up of (a) near the minimum of F . For better visibility, not all SA-points are shown in (a) and (b). (c) Execution time (in seconds) as a function of σ for LM (squares) and SA (circles).

Figure 5a shows a plot of the energy, i.e. the distance

$$dF = F(p_i) - F_0(p_{i,0}) \quad (11)$$

where $F_0(p_{i,0})$ is the value found when taking the true parameter values, as a function of the Euclidean distance $dr = ||p_i - p_{i,0}||_2$ of the parameters from the true parameters values. Apparently, the energy is strongly asymmetrical in at least one of the parameters, which is in agreement with Ref. [18]. Also, the existence of local minima, which apparently attract the LM algorithm, is confirmed. Figure 5b shows a close-up near the lowest minimum to emphasize the higher accuracy of the final result for SA (circles) compared with LM (squares). In this example, it can be seen that the LM algorithm does not converge to the global minimum but deviates shortly before.

Another argument in favor of the SA algorithm is that the execution time approximately 100 s lower than for the LM method, as shown in Fig. 5c. Additionally, whereas the LM algorithm needs to execute on 10 realizations of the time series in order to produce a reasonably accurate result, the SA algorithm was found to converge to the global minimum in almost all instances, implying that fewer realizations are needed for averaging.

4. Discussion and Conclusions

We describe the improvement of a nonparametric procedure to extract measurement noise in empirical stochastic series with strong measurement noise by applying a simulated annealing approach for the optimization step. Simulated annealing accurately extracts the strength of measurement noise and the values of the parameters representing drift and diffusion. These parameters fully describe the evolution equation for the measured quantity. SA produces more reliable and accurate results than a previously used Levenberg-Marquardt algorithm, with the additional benefit of being significantly faster.

Nonparametric reconstruction of the Langevin Eq. (1) from measured stationary data sets merely requires that the process exhibits Markovian properties and fulfills the Pawula theorem [6], whereas the measurement noise needs to be uncorrelated. The Pawula constraint can be relaxed extending the analysis to Lévy noise [23, 24]. It should be pointed out that the method presented here relies solely on

the Markovian properties of the underlying, undisturbed process $x(t)$, and does not require the measured process $y(t)$ to be Markovian.

An extension of this work to multidimensional Langevin time series will be essential for assessing the complexity behind EEG time series or earthquake data. It is likely that we may combine this denoising approach with the method of eigendirections presented in [25].

Acknowledgments

The authors thank D. Kleinhans, M. Wächter, J. Peinke and B. Lehle for useful discussions. They also wish to thank *Fundação para a Ciência e a Tecnologia* (FCT) for the *Ciência 2007* support (PGL), for the fellowship SFRH/BPD/65427/2009 (FR), and for the BII student support (JC). To FCT and *Deutscher Akademischer Austauschdienst* (DAAD) the authors express their gratitude for support through the bilateral cooperation DREBM/DAAD/03/2009 between Portugal and Germany. Finally, they are indebted to the organizers and participants of Dynamics Days 2010 South America for useful discussions in an inspiring atmosphere.

References

- [1] R. Friedrich and J. Peinke, Phys. Rev. Lett. **78**, 863 (1997).
- [2] A.P. Nawroth, J. Peinke, D. Kleinhans, R. Friedrich, Phys. Rev. E **76**, 056102 (2007).
- [3] A. van Mourik A, A. Daffertshofer, P. Beek, Biological Cybernetics **94**, 233(2006).
- [4] R. Friedrich, J. Peinke and Ch. Renner, Phys. Rev. Lett. **84**, 5224 (2000).
- [5] C. Collette and M. Ausloos, Int. J. Mod. Phys. C **15**, 1353 (2004).
- [6] P.G. Lind, A. Mora, J.A.C. Gallas and M. Haase, Phys. Rev. E **72**, 056706 (2005).
- [7] J. Prusseit and K. Lehnertz, Phys. Rev. E **77**, 041914 (2008).
- [8] D. Lamouroux, and K. Lehnertz, Phys. Lett. A **373** 3507 (2009).
- [9] M. Ragwitz and H. Kantz, Phys. Rev. Lett. **87**, 254501 (2001).
- [10] R. Friedrich, Ch. Renner, M. Siefert, and J. Peinke, Phys. Rev. Lett. **89**, 149401 (2002).
- [11] D. Kleinhans, R. Friedrich, A. Nawroth, J. Peinke, Phys. Lett. A **346**, 42-46 (2005).
- [12] J. Gottschall and J. Peinke, New J. Physics **10**, 083034 (2008).
- [13] C. Anteneodo and R. Riera, Phys. Rev. E **80**, 1 (2009).
- [14] H. Kantz and T. Schreiber, *Nonlinear Time Series Analysis*, (Cambridge University Press, Cambridge, England, 1997).
- [15] H.D.I. Abarbanel, R. Brown, J.J. Sidorowich, L.S. Tsimring, Rev. Mod. Phys. **65** 1330 (1993).
- [16] B. Lehle, M. Haase, "Extracting noise and process-parameters from noisy time series", in preparation, 2010.
- [17] F. Boettcher, J. Peinke, D. Kleinhans, R. Friedrich, P.G. Lind, M. Haase, Phys. Rev. Lett. **97** 090603 (2006).
- [18] P. G. Lind, M. Haase, J. Peinke, D. Kleinhans, and R. Friedrich, Phys. Rev. E **81**,1 (2010).
- [19] S. Kirkpatrick, C.D. Gelatt, and M.P. Vecchi, Science **220**, 671 (1983).
- [20] D. Kleinhans, R. Friedrich, M. Wächter and J. Peinke, Phys. Rev. E **76**, 041109 (2007).
- [21] M. Siefert, A. Kittel, R. Friedrich and J. Peinke, Europhys. Lett. **61** 466 (2003).
- [22] W.H. Press, B.P. Flannery, S.A. Teukolsky and W.T. Vetterling, *Numerical Recipes* (Cambridge University Press, Cambridge, 1992).
- [23] R. Friedrich, J. Peinke and M.R.R. Tabar, *Complexity in the view of stochastic processes in Springer Encyclopedia of Complexity and Systems Science* (Springer, Berlin, 2008).
- [24] S. Siegert and R. Friedrich, Phys. Rev. E **64**, 041107 (2001).
- [25] V. Vasconcelos, F. Raischel, M. Haase, D. Kleinhans, J. Peinke and P. G. Lind, in preparation (2011).

